

# Effective therapy of human lymphoma xenografts with a novel recombinant ribonuclease/anti-CD74 humanized IgG<sub>4</sub> antibody immunotoxin

Chien-Hsing Chang, Puja Sapra, Sailaja S. Vanama, Hans J. Hansen, Ivan D. Horak, and David M. Goldenberg

**Ranpirnase (Rap)** is a cytotoxic ribonuclease (RNase) isolated from frog oocytes. Here we describe high antitumor activity of a novel immunotoxin, 2L-Rap-hLL1- $\gamma$ 4P, composed of 2 Rap molecules, each fused to the N terminus of the light chain of hLL1, an internalizing anti-CD74 humanized antibody. To reduce unwanted side effects, the constant region of hLL1 was changed from  $\gamma$ 1 to  $\gamma$ 4 and further to  $\gamma$ 4P by replacing serine<sup>228</sup> to proline to prevent the formation of a half immunoglobulin G (IgG) common

for IgG<sub>4</sub>. In vitro, 2L-Rap-hLL1- $\gamma$ 4P retained RNase activity, specific binding to CD74, and was significantly more potent against CD74<sup>+</sup> cell lines (Daudi, Raji, and MC/CAR) than naked hLL1. In vivo, the pharmacokinetic profile of 2L-Rap-hLL1- $\gamma$ 4P was similar to that of naked hLL1. The maximum tolerated dose of 2L-Rap-hLL1- $\gamma$ 4P in severe combined immunodeficient mice (SCID) or BALB/c mice was 50  $\mu$ g per mouse. In Raji and Daudi Burkitt lymphoma xenograft models, treatment with a single 5 to 50  $\mu$ g

dose of 2L-Rap-hLL1- $\gamma$ 4P, given as early or delayed treatment, resulted in cures of most animals. Treatment with 2L-Rap-hLL1- $\gamma$ 4P was significantly better than all controls, including saline, naked hLL1, and nonspecific immunotoxin. In conclusion, 2L-Rap-hLL1- $\gamma$ 4P demonstrated excellent in vitro and in vivo efficacy and thus merits further consideration as a therapeutic for CD74<sup>+</sup> tumors. (Blood. 2005;106:4308-4314)

© 2005 by The American Society of Hematology

## Introduction

Ranpirnase (Rap), a monomeric protein (*Mr*, 11 817; 104 amino acids), is an amphibian ribonuclease (RNase) belonging to the RNase A superfamily.<sup>1</sup> Native Rap, isolated from *Rana pipiens* eggs,<sup>2</sup> demonstrated significant cytostatic and cytotoxic effects on a variety of tumor cell lines in vitro<sup>3</sup> and in vivo.<sup>4</sup> Rap has a low affinity (more than 1  $\mu$ M) for RNase inhibitor (RI), which constitutes about 0.01% of the cytosolic protein in mammalian cells,<sup>1</sup> and therefore could evade inactivation by RI. As indicated by its resistance to both protease degradation and denaturation at elevated temperatures,<sup>5</sup> Rap is highly stable. Its enzymatic activity requires an N-terminal pyroglutamyl residue.<sup>6</sup> Recombinant Rap (rRap) expressed in *Escherichia coli* with methionine (Met) at the N terminus (Met [-1]) displays much reduced activity,<sup>7</sup> but glycosylation of rRap (expressed in *Pichia pastoris*) increases its conformational stability and toxicity to cancer cells.<sup>8</sup>

Rap enters cells via receptor-mediated endocytosis.<sup>9</sup> Once internalized into the cytosol, it selectively degrades tRNA,<sup>10,11</sup> resulting in inhibition of protein synthesis and induction of apoptosis.<sup>10</sup> Immunotoxins consisting of Rap and LL2, an internalizing anti-CD22 murine monoclonal antibody (mAb),<sup>12</sup> have been prepared by chemical conjugation and shown to have potent and specific antitumor effects against CD22<sup>+</sup> cells both in vitro and in vivo.<sup>13</sup> Rap was studied in the treatment of patients with unresectable malignant mesothelioma,<sup>14</sup> where the reversible dose-limiting toxicity was renal and where there appeared to be no immunogenicity.<sup>15</sup> These encouraging results prompted us to develop a series of novel recombinant immunotoxins involving Rap and other internalizing mAbs.<sup>16,17</sup>

CD74 (invariant chain, Ii) is a type II transmembrane glycoprotein that associates with the major histocompatibility complex (MHC) class II  $\alpha$  and  $\beta$  chains and directs the transport of the  $\alpha\beta$ Ii complexes to endosomes<sup>18</sup> and lysosomes,<sup>19</sup> where Ii is removed via proteolytic cleavage.<sup>19,20</sup> The Ii-free MHC class II molecules subsequently bind antigenic peptides<sup>21</sup> and appear on the cell surface for presentation to CD4<sup>+</sup> T lymphocytes.<sup>22</sup> We have shown previously that CD74<sup>+</sup> cells internalize and catabolize approximately  $8 \times 10^6$  molecules of a murine anti-CD74 mAb (LL1) per cell per day.<sup>23</sup> Because of this rapid internalization, drug conjugates and radiolabeled preparations of LL1 have shown considerable promise as therapeutic agents.<sup>24-27</sup> We have also demonstrated the high expression of the CD74 antigen on a variety of non-Hodgkin lymphoma (NHL) and multiple myeloma clinical specimens and cell lines.<sup>28,29</sup> Also, the acute safety of naked and doxorubicin-conjugated hLL1 was established in cynomolgus monkeys.<sup>27,30</sup> Hence, CD74-directed therapeutics could be an effective strategy for treating hematologic malignancies.

To our knowledge, this is the first report of a recombinantly engineered, purified, immunoglobulin G (IgG)-RNase fusion protein that shows excellent therapeutic activity in vitro and in vivo in human B-cell lymphoma models.

## Materials and methods

### Cell lines

B13-24 and Sp2/0-Ag14 were obtained from American Type Culture Collection ([ATCC] Manassas, VA), and NS0 (ECACC no. 85110503) was

From the Immunomedics, Morris Plains, NJ, and the Garden State Cancer Center, Center for Molecular Medicine and Immunology, Belleville, NJ.

Submitted March 14, 2005; accepted August 11, 2005. Prepublished online as *Blood* First Edition Paper, August 18, 2005; DOI 10.1182/blood-2005-03-1033.

All authors have declared a financial interest or are employed by a company (Immunomedics, Inc) whose potential product was studied in the present work.

**Reprints:** David M. Goldenberg, Garden State Cancer Center, Center for Molecular Medicine and Immunology, 520 Belleville Ave, Belleville, NJ 07109; e-mail: dmg.gscancer@att.net.

The publication costs of this article were defrayed in part by page charge payment. Therefore, and solely to indicate this fact, this article is hereby marked "advertisement" in accordance with 18 U.S.C. section 1734.

© 2005 by The American Society of Hematology

from the European Collection of Cell Cultures (Salisbury, Wiltshire, United Kingdom). Culture media and supplements were purchased from Invitrogen (Carlsbad, CA). Human Burkitt lymphomas (Daudi and Raji), multiple myeloma (MC/CAR), and small cell lung cancer (DMS 53) cell lines were obtained from ATCC. Daudi or Raji cells were grown as suspension cultures in a humidified 37°C incubator with a 5% CO<sub>2</sub> atmosphere in RPMI 1640 medium supplemented with 10% (vol/vol) fetal bovine serum (FBS), penicillin G (100 U/mL), streptomycin sulfate (100 µg/mL), and L-glutamine (2 mM). MC/CAR cells were grown under the same conditions, except that 20% FBS was used. DMS 53 cells were grown adherently in Dulbecco modified Eagle medium (DMEM) supplemented with 10% FBS, penicillin G (100 U/mL), streptomycin sulfate (100 µg/mL), L-glutamine (4 mM), nonessential amino acids (0.1 mM), and sodium pyruvate (1 mM). Only cells in the exponential phase of growth were used for experimentation.

### Animals

Female BALB/c or severe combined immunodeficient mice (SCID) (C.B-17) mice were purchased from Taconic Farms (Germantown, NY). All animal studies were approved by the Center for Molecular Medicine and Immunology's Institutional Animal Care and Use Committee and conducted in compliance with Association of Assessment and Accreditation of Laboratory Animal Care, US Department of Agriculture, and Department of Health and Human Services regulations.

### Antibodies and enzymes

Horseshoe peroxidase (HRP)-conjugated goat anti-human IgG<sub>4</sub> and HRP-conjugated goat anti-mouse Fc antibodies were obtained from Jackson ImmunoResearch Labs (West Grove, PA). Mouse anti-Rap antibodies, rRap, WP (rat anti-id mAb to hLL1), hLL1, hLL1-γ4P, HRP-conjugated LL1, and hLL2 (anti-CD22 humanized antibody, epratuzumab) were prepared in-house. N-glycosidase and all restriction endonucleases were obtained from New England Biolabs (Beverly, MA).

### Construction of IgG<sub>4</sub> constant region containing a proline mutation

Genomic DNA containing the human IgG<sub>4</sub> sequence was isolated from B13-24 cells as follows. Cells were washed with phosphate-buffered saline (PBS), resuspended in digestion buffer (100 mM NaCl, 10 mM Tris [tris(hydroxymethyl)aminomethane]-HCl, 25 mM EDTA [ethylenediaminetetraacetic acid], pH 8.0, 0.5% sodium dodecyl sulfate [SDS], 0.1 mg/mL proteinase K), and incubated at 50°C for 18 hours. A sample was extracted with an equal volume of phenol/chloroform/isoamyl alcohol and precipitated with 7.5 M NH<sub>4</sub>Ac/100% EtOH. Genomic DNA was recovered by centrifugation and dissolved in 50 mM Tris/10 mM EDTA, pH 8.0. Using genomic DNA as a template, the IgG<sub>4</sub> gene was amplified by PCR with suitable primers. The amplified PCR product was cloned in the TOPO-TA cloning vector (Invitrogen) and confirmed by DNA sequencing. *SacII-EagI* fragment containing the heavy chain constant region of IgG<sub>1</sub> in the expression vector *hLL2-pdHLL2*<sup>31</sup> was replaced with *SacII-EagI* of TOPO-TA-IgG<sub>4</sub> plasmid to obtain the vector *pdHLL2-hLL2-γ4*. The mutation (S228P) was then introduced into *pdHLL2-hLL2-γ4* by replacing *PstI-StuI* fragment with a synthetic *PstI-StuI* fragment (56 bp) containing the mutated sequence, resulting in the vector *pdHLL2-hLL2-γ4P*.

### Construction of *pdHLL2-hLL1-γ4P* and *pdHLL2-Rap-L-hLL1-γ4P*

The *XbaI-HindIII* fragment of *pdHLL2-hLL2-γ4P* was replaced with the *XbaI-HindIII* fragment of *pdHLL2-hLL1*<sup>28</sup> containing V<sub>K</sub> and V<sub>H</sub> regions to obtain the vector *pdHLL2-hLL1-γ4P*. A flexible linker (GGGGG)<sub>3</sub> was used to attach the C terminus of Rap to the N terminus of V<sub>K</sub> of hLL1. *XbaI-EcoRV* fragment containing Leader-Rap-Linker was generated and cloned into an intermediate vector to give *pBS-Rap*. Another fragment containing V<sub>K</sub> of hLL1, *EcoRV-BamHI*, was constructed and ligated into *pBS-Rap* to obtain *pBS-Rap-L-hLL1*. Finally, the *XbaI-BamHI* fragment of *pdHLL2-hLL1-γ4P* was replaced with the *XbaI-BamHI* fragment

(*XbaI-Leader-Rap-Linker-Vk-BamHI*) of *pBS-Rap-L-hLL1* to obtain *pdHLL2-Rap-L-hLL1-γ4P*.

### Transfection and screening

The vector DNA (30 µg) was linearized with *Sall* enzyme and transfected into NS0 (4 × 10<sup>6</sup>/mL) or Sp2/0-Ag14 (5 × 10<sup>6</sup>/mL) myeloma cells by electroporation (450 V). Cells were grown in complete hybridoma-SFM supplemented with low IgG, FBS (10%), penicillin G (100 U/mL), streptomycin sulfate (100 µg/mL), L-glutamine (2 mM), sodium pyruvate (1 mM), nonessential amino acids (0.1 mM), and methotrexate (0.1 µM). Positive clones were identified by enzyme-linked immunosorbent assay (ELISA). Briefly, plates were coated with 50 µL of an anti-Rap antibody at 5 µg/mL in PBS and incubated at 4°C overnight. After washing the plate with PBS and blocking with 2% bovine serum albumin (BSA), cell culture supernatants were added. HRP-conjugated goat anti-human IgG<sub>4</sub> antibodies and *o*-phenylenediamine (Sigma, St Louis, MO) were used for detection. Plates were read at 490 nm.

### Expression and purification

Cells were grown to terminal culture (10% to 20% viability) in roller bottles with 500 mL media in each. Culture supernatant was filtered and applied to a protein A column preequilibrated with a pH 8.5 buffer containing 20 mM Tris-HCl and 100 mM NaCl. Following loading, the column was washed with 100 mM sodium citrate, pH 7.0, and eluted with 100 mM sodium citrate, pH 3.5, to obtain the fusion protein. The peak containing the product was adjusted to pH 7.0 using 3 M Tris-HCl, pH 8.5, and dialyzed against PBS. Following concentration, the product was filtered through a 0.22 µm filter and stored at 2°C to 8°C.

### In vitro characterization

Protein purity and concentration were analyzed by size-exclusion high-performance liquid chromatography (SE-HPLC) on a Beckman System Gold Model 116 with a Bio-Sil SEC 250 column purchased from Bio-Rad (Hercules, CA). SDS-polyacrylamide gel electrophoresis (SDS-PAGE) was performed under reducing conditions using PAGEr Gold Precast Gels (Cambrex, East Rutherford, NJ). Matrix-assisted laser desorption ionization time-of-flight (MALDI-TOF) mass spectrometry was performed at the Scripps Research Institute (La Jolla, CA). Two samples of 2L-Rap-hLL1-γ4P were sent for mass analysis—one in native state (1.6 mg/mL in 10 mM PBS) and the other in reduced state (1.6 mg/mL in a pH 7.5 buffer containing 1 mM HEPES [*N*-2-hydroxyethylpiperazine-*N'*-2-ethanesulfonic acid] and 10 mM dithiothreitol). For Western blotting, samples from reducing SDS-PAGE gels were electrotransferred onto PVDF-Plus membranes (GE Osmonics Labstore, Minnetonka, MN). After blocking with 5% BSA, a mouse anti-Rap antibody was added at 1:10 000 dilution or 100 ng/mL and incubated for 1 hour. After washing, HRP-conjugated goat anti-mouse Fc antibodies were added and incubated for 1 hour. Following washing 6 times, LumiGlo substrate (Kirkegaard & Perry Laboratories, Gaithersburg, MD) was added and Kodak film was developed. N-glycosidase treatment was according to the manufacturer's instructions. Samples were denatured by boiling in 0.5% SDS (wt/vol) containing 1% (vol/vol) 2-mercaptoethanol for 10 minutes and incubated with the enzyme for 30 hours at 37°C. After treatment, samples were analyzed by SDS-PAGE. RNase activity was tested by TNT Quick Coupled Transcription/Translation System using the Bright-Glo Luciferase Reporter Assay system according to the supplier's recommendations (Promega, Madison, WI). Test samples were prepared in different dilutions, and 5 µL of each was mixed with 20 µL TNT master mix and incubated for 2 hours at 30°C in a 96-well plate from which 1 µL was removed for analysis with 50 µL Bright-Glo substrate. The affinity of 2L-Rap-hLL1-γ4P, hLL1, hLL1-γ4P, or hLL2 (CD22 control mAb) for WP was evaluated by a competition-binding assay. Briefly, 96-well plates were coated with 50 µL WP (5 µg/mL) and incubated at 4°C overnight. Samples prepared in different 2 × dilutions (final concentrations ranged between 0.49 and 1000 nM) were mixed with an equal volume of 2 × HRP-conjugated

murine hLL1 antibody (final dilution, 1:20 000), added to each well, and incubated for 1 hour. After washing, *o*-phenylenediamine was added and the plates were read at 490 nm. In vitro cytotoxicity was determined using the MTS Cell Titer 96 aqueous one-solution cell proliferation assay (Promega) as follows. CD74<sup>+</sup> cells (Daudi, Raji, MC/CAR) or CD74<sup>-</sup> cells (DMS 53), 20 000 in 0.1 mL, were placed in each well of a 96-well plate and incubated with increasing concentrations of 2L-Rap-hLL1- $\gamma$ 4P or an irrelevant immunotoxin, 2L-Rap-hRS7,<sup>17</sup> for a total of 72 hours. At the end of the incubation, MTS dye was added, and following an additional 2 to 3 hours at 37°C, the plates were read in an Envision plate reader (Perkin Elmer, Boston, MA) at 490 nm.

### Pharmacokinetics and biodistribution

Naked hLL1 or 2L-Rap-hLL1- $\gamma$ 4P was conjugated to diethylenetriamine-pentaacetic acid (DTPA) using 2-(4-isothiocyanatobenzyl)DTPA (Macrocyclics, Dallas, TX), as described by Sharkey et al,<sup>32</sup> to obtain DTPA-hLL1 or DTPA-2L-Rap-hLL1- $\gamma$ 4P, which was labeled with <sup>88</sup>Y chloride (Los Alamos National Laboratory, Los Alamos, NM) or <sup>111</sup>In chloride (Perkin Elmer), respectively, for pharmacokinetic studies. Naive female SCID mice (8 weeks old, 18 to 22 g) were injected intravenously with a mixture of 0.001 mCi (0.037 MBq) <sup>88</sup>Y-DTPA-hLL1 and 0.02 mCi (0.74 MBq) <sup>111</sup>In-DTPA-2L-Rap-hLL1- $\gamma$ 4P, supplemented with unlabeled DTPA conjugates of hLL1 or 2L-Rap-hLL1- $\gamma$ 4P, so that each animal received a total dose of 10  $\mu$ g each of hLL1 and 2L-Rap-hLL1- $\gamma$ 4P. At selected times after dosing (1, 2, 4, 16, 48, 72, and 168 hours), groups of 5 mice were anesthetized and a blood sample withdrawn by cardiac puncture. Blood samples were counted in a calibrated gamma counter, Minaxi  $\lambda$  Auto-Gamma 5000 series gamma counter (Packard Instruments, Downers Grove, IL) for <sup>111</sup>In (channels 120 to 480) and <sup>88</sup>Y (channels 600 to 2000). A crossover curve was generated to correct for the back scatter of <sup>88</sup>Y energy into the <sup>111</sup>In counting window.

### In vivo toxicity

Naive SCID or BALB/c mice were injected intravenously with various doses of 2L-Rap-hLL1- $\gamma$ 4P ranging from 25 to 400  $\mu$ g per mouse and were monitored daily for visible signs of toxicity and body weight change. The maximum tolerated dose (MTD) was defined as the highest dose at which no death occurred, and body weight loss was 20% or less of pretreatment animal weight (approximately 20 g). Animals that experienced toxic effects were killed, necropsied, and subjected to clinical chemistry and histopathological analysis.

### Therapeutic efficacy in tumor-bearing mice

Female SCID mice (8 weeks old, 18 to 22 g), 7 to 10 per group, were injected intravenously with either  $1.5 \times 10^7$  Daudi cells or  $2.5 \times 10^6$  Raji cells. Therapeutics were injected 1, 6, 10, or 15 days after inoculation of the tumor cells. Mice were examined daily for hind-leg paralysis and were weighed weekly. The animals were killed when they developed hind-leg paralysis or lost more than 20% of their pretreatment weight.

### Data analysis

In vitro cytotoxicity studies, dose-response curves were generated from the mean of triplicate determinations, and 50% inhibitory concentration (IC<sub>50</sub>) values were obtained using the GraphPad Prism software (Advanced Graphics Software, Encinitas, CA). Pharmacokinetic data were analyzed using the standard algorithms of noncompartmental analysis program WinNonlin, Version 4.1 (Pharsight, Mountain View, CA). The program calculates area under the curve (AUC) using the linear trapezoidal rule with a linear interpolation. The elimination rate constant ( $k_{el}$ ) was computed from the terminal half-life ( $t_{1/2\beta}$ ), assuming first-order kinetics. Survival studies were analyzed using Kaplan-Meier plots (log-rank analysis) with GraphPad Prism software. Differences were considered significant at *P* less than .05.

## Results

### Expression, purification, and characterization of 2L-Rap-hLL1- $\gamma$ 4P

The Rap-fused recombinant immunotoxin was readily recovered from culture supernatants following purification on protein A. On SE-HPLC, a sharp single peak was observed at 7.6 minutes, as shown in Figure 1A, with the retention time indicating the molecule was larger than IgG. On reducing SDS-PAGE (Figure 1B), a band related to the heavy chain of expected size (*M<sub>r</sub>* about 50 000) and 2 bands of *M<sub>r</sub>* about 37 000 and 39 000, both larger than the light chain of hLL1 (*M<sub>r</sub>* about 25 000), were observed. MALDI-TOF mass spectrometry of the unreduced sample showed one major peak of 177 150, which is in good agreement with the molecular mass of 1 IgG (*M<sub>r</sub>* about 150 000) plus 2 Rap molecules (*M<sub>r</sub>* about 24 000) (data not shown). The reduced sample showed 3 major peaks at 50 560 (corresponding to the heavy chain), 38 526, and 36 700 (corresponding to the 2 light chains containing Rap). Western blotting confirmed the presence of Rap on both light chains, as shown in Figure 2A. Because Rap has a potential N-glycosylation site (Asn-X-Thr/Ser) at N69, the observation of 2 light chains with a molecular mass difference of 2000 could be the result of uneven glycosylation of Rap. To investigate this possibility, the product purified by protein A was incubated with N-glycosidase under denatured conditions. As shown in Figure 2B, after N-glycosidase treatment the 2 bands corresponding to the 2 light chains converged into 1 (the faster migrating band), thus demonstrating that glycosylation of Rap was the most likely cause for the 2 bands observed on SDS-PAGE. Further support was provided by the observation of only 1 Rap-fused light chain when Rap(N69Q), a variant of Rap with the glycosylation site removed, is substituted for Rap in the recombinant construct (data not shown).<sup>16</sup>

### Functional properties

RNase activity was determined using an in vitro transcriptional/translational (IVTT) assay that measured inhibition of protein synthesis due to mRNA degradation. As shown in Figure 3,

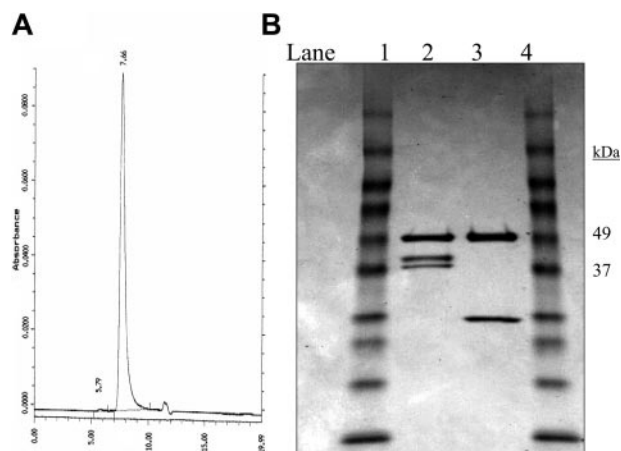


**Figure 1. Characterization of 2L-Rap-hLL1- $\gamma$ 4P.** (A) SE-HPLC trace. A single peak was observed at 7.6 minutes, which was shorter than the retention time observed for hLL1 (about 8 minutes). (B) Reducing SDS-PAGE analysis. Lanes 1 and 4: *M<sub>r</sub>* markers; lane 2: 2L-Rap-hLL1- $\gamma$ 4P; lane 3: IgG. Two closely migrating bands attributed to the fused light chains, both larger than the light chain of hLL1, are observed in lane 2.



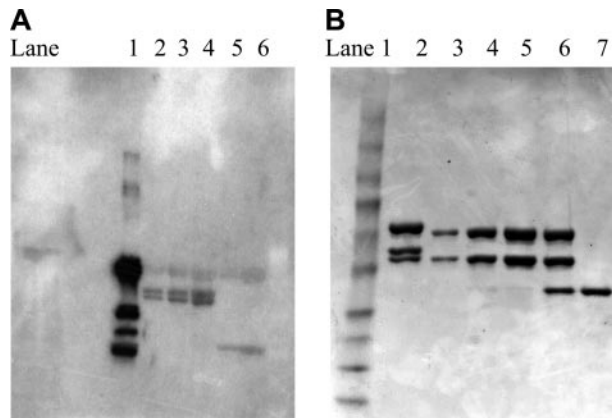


**Figure 2. Presence of Rap on the light chain and glycosylation.** (A) Western blotting. Lane 1: anti-Rap mAb; lanes 2 to 4: 2L-Rap-hLL1- $\gamma$ 4P in increasing amounts; lanes 5 to 6: hLL1. Two bands corresponding to the fused light chains of 2L-Rap-hLL1- $\gamma$ 4P were clearly detected in lanes 2 to 4 by a mouse anti-Rap mAb, indicating the presence of Rap on both light chains. (B) N-glycosidase treatment of 2L-Rap-hLL1- $\gamma$ 4P. Lane 1: Mr markers; lane 2: untreated sample; lanes 3 to 5: samples treated with excess N-glycosidase loaded in increasing amounts; lane 7: untreated sample.

2L-Rap-hLL1- $\gamma$ 4P had an  $IC_{50}$  value of 269 pM, which was approximately 2-fold higher than that of rRap (113 pM); no activity was detected for hLL1- $\gamma$ 4P. That the affinity of 2L-Rap-hLL1- $\gamma$ 4P for WP was unaltered compared with that of hLL1 or hLL1- $\gamma$ 4P is indicated by the indistinguishable binding curves shown in Figure 4; the irrelevant anti-CD22 mAb, hLL2, has no affinity at all.

The in vitro cytotoxicity of 2L-Rap-hLL1- $\gamma$ 4P was evaluated on 3 CD74<sup>+</sup> (Daudi, Raji, and MC/CAR) and 1 CD74<sup>-</sup> cell line (DMS 53) (Table 1). 2L-Rap-hLL1- $\gamma$ 4P displayed strong cytotoxicity against all 3 CD74<sup>+</sup> cell lines, whereas the irrelevant 2L-Rap-hRS7 showed little or no cytotoxicity under the same conditions. The  $IC_{50}$  values of 2L-Rap-hLL1- $\gamma$ 4P for Daudi, MC/CAR, and Raji following a 3-day exposure at 37°C were 0.6, 0.6, and 1.3 nM, respectively. 2L-Rap-hRS7 demonstrated little or no cytotoxicity, and the specificity ratio (defined as  $IC_{50}$  value of 2L-Rap-hRS7/ $IC_{50}$  value of 2L-Rap-hLL1- $\gamma$ 4P) was 794-fold, more than 430-fold, and more than 888-fold for Daudi, Raji, and MC/CAR cells, respectively. Naked hLL1 did not display significant cytotoxicity at the concentrations tested. In the CD74<sup>-</sup> cell line (DMS 53), the  $IC_{50}$  was not reached for 2L-Rap-hLL1- $\gamma$ 4P and 2L-Rap-hRS7 up to the highest concentration tested (560 nM).

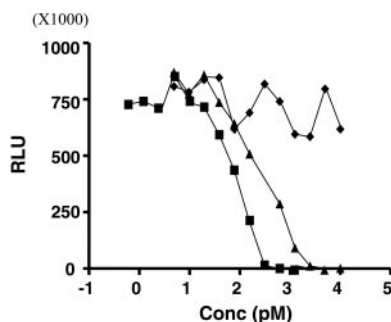


**Figure 3. RNase activity as measured by the in vitro transcription/translation (IVTT) assay.** Increasing concentrations of protein samples were incubated with IVTT reagent mixture containing luciferase plasmid DNA and analyzed with luciferase assay reagent. Samples containing active RNase inhibit synthesis of luciferase mRNA. Concentrations of rRap (■), 2L-Rap-hLL1- $\gamma$ 4P (▲), and hLL1- $\gamma$ 4P (◆) were plotted against relative luminescence units (RLU).

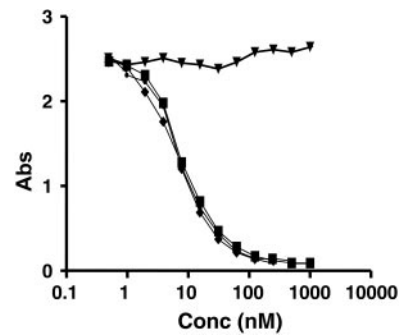


**Figure 4. Competition binding for WP.** The binding affinity of each test article for WP was compared with HRP-mLL1 in a competition ELISA using plates coated with WP. Concentrations of 2L-Rap-hLL1- $\gamma$ 4P (■), hLL1- $\gamma$ 4P (◆), hLL1 (●), and hLL2 (▼) were plotted against absorbance at 490 nm.

### Pharmacokinetic and biodistribution data

The pharmacokinetics of radiolabeled hLL1 mAb and 2L-Rap-hLL1- $\gamma$ 4P were determined in naive (tumor-free) SCID mice. hLL1 and 2L-Rap-hLL1- $\gamma$ 4P were conjugated with DTPA and trace-labeled with  $^{88}Y$  and  $^{111}In$ , respectively. The radiolabeled substrates were found to be immunoreactive after mixing mAb with WP, the anti-idiotype mAb to hLL1, and analyzing by SE-HPLC with radiometric detection. Figure 5 presents the blood clearance profile of  $^{111}In$ -DTPA-2L-Rap-hLL1- $\gamma$ 4P versus  $^{88}Y$ -DTPA-hLL1 in mice. Radiolabeled 2L-Rap-hLL1- $\gamma$ 4P had a pharmacokinetic profile similar to that of radiolabeled mAb hLL1. Both hLL1 mAb and 2L-Rap-hLL1- $\gamma$ 4P had a biphasic clearance from the circulation, characterized by an initial rapid redistribution ( $\alpha$ ) and a later slower clearance ( $\beta$ ) phase. A slightly shorter  $\alpha$  half-life was observed for 2L-Rap-hLL1- $\gamma$ 4P (5.1 hours) compared with hLL1 (4 hours). Data points beyond 5 hours were used to compute the terminal half-life ( $t_{1/2\beta}$ ) and elimination rate constant ( $k_{\beta}$ ). The  $t_{1/2\beta}$  of hLL1 and 2L-Rap-hLL1- $\gamma$ 4P was 103 hours and 113 hours, respectively. 2L-Rap-hLL1- $\gamma$ 4P had a mean residence time (MRT) similar to that of hLL1 (156 hours for 2L-Rap-hLL1- $\gamma$ 4P versus 140 hours for hLL1). The rate of clearance (Cl) of both 2L-Rap-hLL1- $\gamma$ 4P and hLL1 was 0.025 mL/h. Thus, 2L-Rap-hLL1- $\gamma$ 4P displayed a pharmacokinetic profile similar to native mAb hLL1.

### In vivo toxicity

In naive SCID and BALB/c mice, a single intravenous dose above 75  $\mu$ g or 100  $\mu$ g 2L-Rap-hLL1- $\gamma$ 4P, respectively, resulted in severe weight loss and death of the animals, but all mice survived a dose of 50  $\mu$ g. Therefore, the MTD of 2L-Rap-hLL1- $\gamma$ 4P given as a single bolus injection is between 50 and 75  $\mu$ g in SCID mice and between 50 and 100  $\mu$ g in BALB/c mice. Gross pathological examination of dead or killed mice indicated that the liver was pale in color and the spleen was shriveled and smaller than the usual size. Histopathological examination revealed hepatic and splenic necrosis. Serum samples of representative mice had elevated levels of alanine aminotransferase, aspartate aminotransferase, and total bilirubin, suggesting significant liver toxicity.

### Therapeutic efficacy in tumor-bearing mice

The therapeutic efficacy of 2L-Rap-hLL1- $\gamma$ 4P was evaluated in human xenograft models of NHL, Daudi, and Raji. In the first experiment, treatment of mice bearing Daudi xenografts with a single injection of 5- to 50- $\mu$ g doses of 2L-Rap-hLL1- $\gamma$ 4P, 1 day

**Table 1. In vitro cytotoxicity of 2L-Rap-hLL1- $\gamma$ 4P against human tumor cell lines**

Cell line	Type	CD74	IC <sub>50</sub> ,* nM			Specificity ratio
			2L-Rap-hLL1- $\gamma$ 4P	Rap-hRS7	hLL1	
Daudi	NHL	+	0.63	500	> 660	794
Raji	NHL	+	1.3	> 560	> 560	> 430
MC/CAR	Multiple myeloma	+	0.63	> 560	> 560	> 888
DMS 53	Small cell lung cancer	-	> 560	> 560	> 560	1

\*Concentration responsible for 50% growth inhibition in MTS dye reduction assay.

after inoculation of cells, resulted in curing 90% of animals out to 180 days after injection of cells (Figure 6A). Notably, treatment with 1  $\mu$ g 2L-Rap-hLL1- $\gamma$ 4P increased the life span of animals by 230% compared with controls. A control group, which received a mixture of hLL1- $\gamma$ 4P (43  $\mu$ g) and Rap (7  $\mu$ g), representing the composition of the component proteins in 50  $\mu$ g 2L-Rap-hLL1- $\gamma$ 4P had a median survival time (MST) of 70 days versus 28 days for the saline group ( $P < .001$ ).

A second study was performed to establish the specific targeting advantage of 2L-Rap-hLL1- $\gamma$ 4P (Figure 6B). SCID mice bearing Daudi xenografts, when treated with a low dose of 15  $\mu$ g 2L-Rap-hLL1- $\gamma$ 4P 1 day after inoculation of cells, resulted in curing 100% of the animals, and this treatment was significantly better than all the control groups ( $P < .001$ ). Treatment with 50  $\mu$ g nonspecific immunotoxin (2L-Rap-hRS7) or with 2  $\mu$ g rRap (2  $\mu$ g rRap dose corresponds to the amount of Rap in 15  $\mu$ g 2L-Rap-hLL1- $\gamma$ 4P) did not improve the survival of mice over those injected with saline. However, treatment with naked hLL1- $\gamma$ 4P at the low dose of 13  $\mu$ g hLL1 (13  $\mu$ g hLL1 dose corresponds to the amount of antibody in 15  $\mu$ g 2L-Rap-hLL1- $\gamma$ 4P) or with a combination of 13  $\mu$ g naked hLL1- $\gamma$ 4P and 2  $\mu$ g rRap resulted in an improvement in life span by 115% and 92%, respectively, compared with mice injected with saline but was significantly less than 2L-Rap-hLL1- $\gamma$ 4P ( $P < .005$ ).

The therapeutic efficacy of 2L-Rap-hLL1- $\gamma$ 4P in relation to tumor burden was also evaluated in another NHL xenograft model (Raji) (Figure 7A). Treatment with 50  $\mu$ g 2L-Rap-hLL1- $\gamma$ 4P at 1 or 6 days after inoculation of tumor cells resulted in curing 5 of 8 and 6 of 8 animals, respectively, observed out to 80 days. However, delaying the treatment to 10 days after injection of tumor cells only increased the MST of animals to 23 days from 16 days for the saline-injected animals ( $P < .001$ ). All animals receiving 50  $\mu$ g of the nonspecific immunotoxin, 2L-Rap-hRS7, or 7  $\mu$ g rRap died with MSTs of 20 and 16 days, respectively. As observed in the Daudi xenograft model, animals receiving naked hLL1 at a dose of

43  $\mu$ g hLL1 or the mixture of naked hLL1 (43  $\mu$ g) and rRap (7  $\mu$ g) had significantly improved life spans compared with animals receiving saline ( $P < .001$ ) but significantly less than the MSTs of animals treated with 2L-Rap-hLL1- $\gamma$ 4P ( $P < .001$ ).

Similar results are being observed in a current study in the Daudi xenograft model involving a delayed therapy. Whereas all animals treated with saline died with an MST of 27 days, groups of animals that received a single injection of 50  $\mu$ g 2L-Rap-hLL1- $\gamma$ 4P at 6, 10, or 15 days after injection of cells have significantly improved life spans at least more than 150% over those injected with saline.

## Discussion

An excellent therapeutic index was achieved in preclinical models of NHL with a newly designed and expressed recombinant fusion protein of RNase and humanized anti-CD74 antibody. We demonstrated that this fusion protein expressed in mouse myeloma cells was full size with no detectable half molecules, glycosylated on Rap, and uncompromised in immunologic and enzymatic activities. Furthermore, the fusion protein with the IgG<sub>4</sub> constant region was found to have similar pharmacokinetic and tissue uptake properties to those of hLL1 with the IgG<sub>1</sub> constant region. Although Rap was inserted at the N terminus of each of the 2 light chains to retain full RNase activity, the binding affinity of the fusion protein was shown to be unaffected by this placement. Other choices, like placing Rap on heavy chains or both the light and heavy chains, are equally attractive. The potent cytotoxic effect of 2L-Rap-hLL1- $\gamma$ 4P was demonstrated in CD74<sup>+</sup> Burkitt NHL (Daudi and Raji) and multiple myeloma cell lines (MC/CAR). The cytotoxic effect of 2L-Rap-hLL1- $\gamma$ 4P was specific, because an irrelevant fusion construct, 2L-Rap-hRS7, which targets epithelial glycoprotein-1,<sup>33</sup> showed little or no cytotoxicity to CD74<sup>+</sup> cells. Moreover, the growth of a CD74<sup>-</sup> cell line (DMS 53) was not affected by 2L-Rap-hLL1- $\gamma$ 4P. Further, we demonstrated an excellent therapeutic index in vivo of 2L-Rap-hLL1- $\gamma$ 4P in 2 animal models of NHL (Raji, Daudi). In 4 therapy experiments of separate xenograft models, high cure rates approaching 100% were achieved with very low doses of 2L-Rap-hLL1- $\gamma$ 4P in early or advanced tumor models. This therapeutic efficacy could be a result of the rapid rate of internalization of the CD74 molecule bound by the immunotoxin and, consequently, the delivery of high amounts of 2L-Rap-hLL1- $\gamma$ 4P intracellularly. It is impressive that treatment with a dose as low as 1  $\mu$ g 2L-Rap-hLL1- $\gamma$ 4P yielded significant survival enhancement, providing greater than a 300% increase in MST. The therapeutic effects were specific, because nonspecific 2L-Rap-hRS7 at the MTD failed to demonstrate any benefit in both the Raji and Daudi models. Treatment with 2L-Rap-hLL1- $\gamma$ 4P was significantly better than treatment with either naked hLL1 or the mixture of hLL1 and rRap, thus

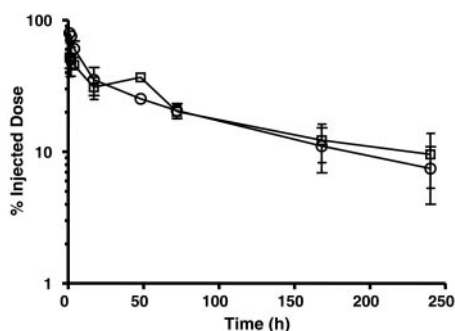


**Figure 5. Blood clearance of 2L-Rap-hLL1- $\gamma$ 4P in naive SCID mice.** Naive SCID mice were coinjected intravenously with <sup>88</sup>Y-DTPA-hLL1 (○) and <sup>111</sup>In-DTPA-2L-Rap-hLL1- $\gamma$ 4P (□). At selected times after dosing, mice were bled by cardiac puncture and a blood sample was counted for radioactivity. Data represent mean  $\pm$  SD of injected dose in blood (n = 3).

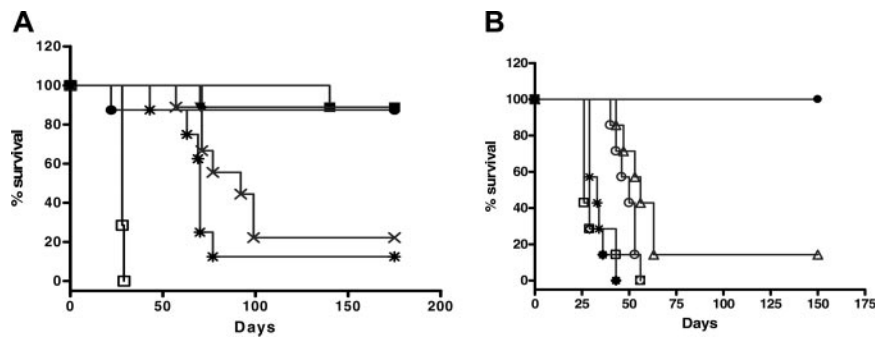


**Figure 6. Therapeutic efficacy of 2L-Rap-hLL1- $\gamma$ 4P in Daudi human xenograft model of NHL.** (A) Treatment of Daudi lymphoma with 2L-Rap-hLL1- $\gamma$ 4P. SCID mice (8 to 10 mice per group) were inoculated intravenously with  $1.5 \times 10^7$  Daudi cells. After 1 day, mice were treated with a single bolus injection of 1  $\mu$ g ( $\times$ ), 5  $\mu$ g ( $\blacksquare$ ), 15  $\mu$ g ( $\blacktriangle$ ), 30  $\mu$ g ( $\blacktriangledown$ ), 40  $\mu$ g ( $\blacklozenge$ ), or 50  $\mu$ g ( $\bullet$ ) of 2L-Rap-hLL1- $\gamma$ 4P. Control groups were injected with component proteins equivalent to 50  $\mu$ g of the immunotoxin (\*) or PBS ( $\square$ ) only. (B) Specific targeting of 2L-Rap-hLL1- $\gamma$ 4P in Daudi lymphoma xenograft model. SCID mice (7 to 8 per group) were inoculated intravenously with  $1.5 \times 10^7$  Daudi cells. After 1 day, mice were treated with a single bolus intravenous injection of 15  $\mu$ g 2L-Rap-hLL1- $\gamma$ 4P ( $\bullet$ ). Control animals received saline ( $\square$ ), 13  $\mu$ g naked hLL1 ( $\circ$ ), 2  $\mu$ g rRap ( $\diamond$ ), a mixture of naked hLL1 and rRap ( $\triangle$ ), and nonspecific immunotoxin 2L-Rap-hRS7 (\*).

supporting the specific therapeutic advantage of the 2L-Rap-hLL1- $\gamma$ 4P immunotoxin.

Rap chemically conjugated to murine LL2 targeting a different antigen (CD22) has shown antitumor activity in 2 SCID mouse xenograft models of human Burkitt lymphoma.<sup>13</sup> In comparison, our therapy results obtained with similar models indicated that 2L-Rap-hLL1- $\gamma$ 4P is significantly more efficacious at lower doses than the Rap-conjugated LL2. The improved therapeutic results observed in our studies at lower doses in the Daudi xenograft model might be attributed to more efficient internalization of 2L-Rap-hLL1- $\gamma$ 4P upon binding to CD74 in vivo. Also, we confirmed these therapeutic results in a second Burkitt lymphoma model, Raji. However, it should be understood that 2L-Rap-hLL1- $\gamma$ 4P targets a different receptor than the Rap-conjugated LL2, thus making the above comparison of in vivo efficacy less relevant because of 2 variables, different antibodies and methods of RNase attachment to hLL1 and murine LL2. Interestingly, our in vivo antitumor efficacy results are very comparable to those reported for BL22,<sup>34</sup> a recombinant immunotoxin in which a disulfide-linked Fv of an anti-CD22 antibody was fused to PE38, a truncated form of *Pseudomonas* exotoxin A.

Our toxicity studies of 2L-Rap-hLL1- $\gamma$ 4P in mouse models demonstrated a nonspecific hepatotoxicity of the immunotoxin but did not suggest any toxicity related to CD74 in normal tissue due to the lack of cross-reactivity of hLL1 with rodent CD74. In an immunohistochemistry study of human specimens of lymph node, spleen, bone marrow, heart, liver, and kidney tissues, we observed hLL1 staining to be consistent with hematopoietic precursors, lymphocytes, dendritic cells, Kupffer cells, endothelial cells, and renal glomeruli (data not shown). The hLL1 mAb, which recognizes human CD74, is cross-reactive with cynomolgus and rhesus monkey tissues. Our preliminary results from tolerability studies in cynomolgus monkeys indicated that naked hLL1 could be administered safely in single doses of up to 125 mg/kg.<sup>30</sup> Future studies will aim to determine the tolerability of 2L-Rap-hLL1- $\gamma$ 4P in monkeys.

Immunogenicity, vascular leak syndrome, and nonspecific liver toxicity are among the major safety concerns of immunotoxins constructed with plant and bacterial toxins.<sup>35,36</sup> For example, severe side effects from vascular leak syndrome have halted clinical trials of ricin immunoconjugates and lead to modification of this molecule to abrogate this undesirable side effect.<sup>37</sup> Because the native sequence of Rap lacks the 3 amino acid sequence motif (x)D(y) identified in toxins and interleukin-2 that is responsible for binding to endothelial cells,<sup>38</sup> it may

be of less concern for Rap-containing immunotoxins with regard to causing vascular leak syndrome,<sup>39</sup> but this will require evaluation. Although Rap can be administered repeatedly to patients without untoward immune responses,<sup>14,15</sup> the immunogenicity of the much larger fusion proteins consisting of Rap and a humanized IgG<sub>4</sub> remains to be determined. Because the Rap-hIgG fusion proteins are highly basic (pI above 10), potential liver toxicity is also a concern based on several studies showing that increased liver toxicity of a *Pseudomonas* immunotoxin could be correlated with its higher pI value<sup>40,41</sup> and as has also been observed at higher doses of the Rap immunotoxin studied here. It has also been suggested that tumor necrosis factor- $\alpha$  (TNF- $\alpha$ ) produced by Kupffer cells is the major cause of liver toxicity of immunotoxins and that this toxicity could be blocked by TNF-binding proteins and nonsteroidal anti-inflammatory drugs (NSAIDs), such as indomethacin, which inhibits TNF- $\alpha$ .<sup>41</sup> The excellent therapeutic index of 2L-Rap-hLL1- $\gamma$ 4P in xenograft models (about 50-fold above hepatotoxic doses) together with the successful clinical studies using *Pseudomonas* immunotoxin<sup>42</sup> suggest that this recombinant RNase immunotoxin should be studied in patients.

Recombinant immunotoxins, as produced by our approach, have several advantages, including simple and scalable purification processes, homogenous and fully functional products, and comparable yields to those of humanized antibodies. Furthermore, the method described can be applied to the construction of

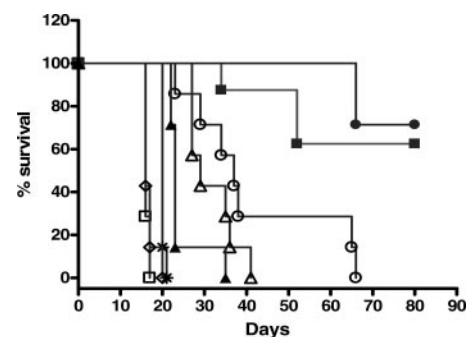


**Figure 7. Therapeutic efficacy of 2L-Rap-hLL1- $\gamma$ 4P in SCID mice bearing Raji cells.** SCID mice (7 to 8 per group) were inoculated intravenously with  $2.5 \times 10^6$  Raji cells. Mice were treated with a single intravenous bolus dose of 50  $\mu$ g 2L-Rap-hLL1- $\gamma$ 4P at 1 day ( $\blacksquare$ ), 5 days ( $\bullet$ ), or 10 days ( $\blacktriangle$ ) after inoculation of cells. Control animals received saline ( $\square$ ), 50  $\mu$ g naked hLL1 ( $\triangle$ ), 7  $\mu$ g rRap ( $\diamond$ ), a mixture of naked hLL1 and rRap ( $\circ$ ), or nonspecific immunotoxin Rap-hRS7 (\*).



a variety of immunconjugates containing different toxin moieties and antigen-specific antibodies that may prove to be clinically useful for the targeted therapy of cancer. In conclusion, we have constructed a CD74-targeted novel recombinant immunotoxin containing 2 molecules that has demonstrated curative therapeutic effects in animal models of human B-cell lymphoma and thus could be a potential therapeutic for CD74<sup>+</sup> lymphomas and myelomas.

## References

- Leland PA, Schultz LW, Kim B-Y, Raines RT. Ribonuclease A variants with potent cytotoxic activity. *Proc Natl Acad Sci U S A*. 1998;95:10407-10412.
- Ardelt W, Mikulski SM, Shogen K. Amino acid sequence of an anti-tumor protein from *Rana pipiens* oocytes and early embryos. *J Biol Chem*. 1991;266:245-251.
- Darzynkiewicz Z, Carter SP, Mikulski SM, Ardelt W, Shogen K. Cytostatic and cytotoxic effects of Pannon (P-30 protein), a novel anticancer agent. *Cell Tissue Kinet*. 1988;21:169-182.
- Mikulski SM, Ardelt W, Shogen K, Berstein EH, Menduke H. Striking increase of survival of mice bearing M109 Madison carcinoma treated with a novel protein from amphibian embryos. *J Natl Cancer Inst*. 1990;82:151-153.
- Notomista E, Catanzano F, Graziano G, et al. Onconase: an unusually stable protein. *Biochemistry*. 2000;39:8711-8718.
- Boix E, Wu Y, Vasandani VM, et al. Role of the N terminus in RNase A homologues: differences in catalytic activity, ribonuclease inhibitor interaction and cytotoxicity. *J Mol Biol*. 1996;257:992-1007.
- Newton DL, Xue Y, Boque L, Wlodawer A, Kung HF, Rybak SM. Expression and characterization of a cytotoxic human-frog chimeric ribonuclease: potential for cancer therapy. *Protein Eng*. 1997;10:463-470.
- Kim B-M, Kim H, Raines RT, et al. Glycosylation of onconase increases its conformational stability and toxicity for cancer cells. *Biochem Biophys Res Commun*. 2004;315:976-983.
- Wu Y, Saxena SK, Ardelt W, et al. A study of the intracellular routing of cytotoxic ribonucleases. *J Biol Chem*. 1995;270:17476-17481.
- Iordanov MS, Ryabinina OP, Wong J, et al. Molecular determinants of apoptosis induced by the cytotoxic ribonuclease onconase: evidence for cytotoxic mechanism different from inhibition of protein synthesis. *Cancer Res*. 2000;60:1983-1994.
- Saxena SK, Sirdeshmukh R, Ardelt W, Mikulski SM, Shogen K, Youle RJ. Entry into cells and selective degradation of tRNAs by a cytotoxic member of the RNase A family. *J Biol Chem*. 2002;277:15142-15146.
- Leung SO, Shevitz J, Pellegrini MC, et al. Chimerization of LL2, a rapidly internalizing antibody specific for B-cell lymphoma. *Hybridoma*. 1994;13:469-472.
- Newton DL, Hansen HJ, Mikulski SM, Goldenberg DM, Rybak SM. Potent and specific antitumor effects of an anti-CD22-targeted cytotoxic ribonuclease: potential for the treatment of non-Hodgkin lymphoma. *Blood*. 2001;97:528-535.
- Mikulski SM, Costanzi JJ, Vogelzang NJ, et al. Phase II trial of a single weekly intravenous dose of ranpirnase in patients with unresectable malignant mesothelioma. *J Clin Oncol*. 2002;20:274-281.
- Mikulski SM, Grossman AM, Carter PW, Shogen K, Costanzi JJ. Phase I human clinical trial of Onconase (P-30 protein) administered intravenously on a weekly schedule in cancer patients with solid tumors. *Int J Oncol*. 1993;3:57-64.
- Vanama SS, Sapra P, Hansen HJ, Horak ID, Goldenberg DM, Chang C-H. Construction and characterization of two recombinant immunotoxins consisting of glycosylated and non-glycosylated ranpirnase fused to an internalizing anti-CD74 humanized IgG4 antibody [abstract]. *Cancer Biother Radiopharm*. 2004;19:514.
- Vanama SS, Sapra P, Hansen HJ, Horak ID, Chang C-H, Goldenberg DM. Construction, characterization, and mammalian expression of an immunotoxin consisting of ranpirnase fused to a humanized anti-EGP-1 antibody, hRS7, as a potential therapeutic for prostate cancer. *Proc Am Assoc Cancer Res*. 2005;46:160. Abstract 679.
- Roche PA, Teletski CL, Stang E, Bakke O, Long EO. Cell surface HLA-DR-invariant chain complexes are targeted to endosomes by rapid internalization. *Proc Natl Acad Sci U S A*. 1993;90:8581-8585.
- Morton PA, Zacheis ML, Giacoletto KS, Manning JA, Schwartz BD. Delivery of nascent MHC class II-invariant chain complexes to lysosomal compartments and proteolysis of invariant chain by cysteine proteases precedes peptide binding in B-lymphoblastoid cells. *J Immunol*. 1995;154:137-150.
- Blum JS, Cresswell P. Role for intracellular proteases in the processing and transport of class II HLA antigens. *Proc Natl Acad Sci U S A*. 1988;85:3975-3979.
- Roche PA, Cresswell P. Proteolysis of the class II-associated invariant chain generates a peptide binding site in intracellular HLA-DR molecules. *Proc Natl Acad Sci U S A*. 1991;88:3150-3154.
- Germain RN, Margulies DH. The biochemistry and cell biology of antigen processing and presentation. *Annu Rev Immunol*. 1993;11:403-450.
- Hansen HJ, Ong GL, Diril H, et al. Internalization and catabolism of radiolabeled antibodies to the MHC class-II invariant chain by B-cell lymphoma. *Biochem J*. 1996;320:293-300.
- Govindan SV, Goldenberg DM, Elsamra SE, et al. Radionuclides linked to a CD74 antibody as therapeutic agents for B-cell lymphoma: comparison of Auger electron emitters with beta-particle emitters. *J Nucl Med*. 2000;41:2089-2097.
- Ochakovskaya R, Osorio L, Goldenberg DM, Mattes MJ. Therapy of disseminated B-cell lymphoma xenografts in severe combined immunodeficient mice with anti-CD74 antibody conjugated with <sup>111</sup>indium, <sup>67</sup>gallium, or <sup>90</sup>yttrium. *Clin Cancer Res*. 2001;7:1505-1510.
- Griffiths GL, Mattes MJ, Stein R, et al. Cure of SCID mice bearing human B-lymphoma xenografts by an anti-CD74 antibody-anthracycline drug conjugate. *Clin Cancer Res*. 2003;9:6567-6571.
- Sapra P, Stein R, Pickett J, et al. Anti-CD74 antibody-doxorubicin conjugate, IMMU-110, in a human multiple myeloma xenograft and in monkeys. *Clin Cancer Res*. 2005;11:5257-5264.
- Stein R, Qu Z, Cardillo T, et al. Anti-proliferative activity of a humanized anti-CD74 monoclonal antibody, hLL1, on B-cell malignancies. *Blood*. 2004;104:3705-3711.
- Burton JD, Ely S, Reddy PK, et al. CD74 is expressed by multiple myeloma and is a promising target for therapy. *Clin Cancer Res*. 2004;10:6606-6611.
- Sapra P, Griffiths GL, Govindan SV, et al. Pharmacokinetics and tissue biodistribution of a doxorubicin-antibody (anti-CD74) conjugate, IMMU-110, in mice and tolerability of naked anti-CD74 in cynomolgus monkeys. *Eur J Cancer Suppl*. 2004;2:88. Abstract 290.
- Losman MJ, Hansen HJ, Dworak H, et al. Generation of a high-producing clone of a humanized anti-B-cell lymphoma monoclonal antibody (hLL2). *Cancer*. 1997;80(suppl):2660-2666.
- Sharkey RM, Motta-Hennessy C, Gansow OA, et al. Selection of a DTPA chelate conjugate for monoclonal antibody targeting to a human colonic tumor in nude mice. *Int J Cancer*. 1990;46:79-85.
- Basu A, Goldenberg DM, Stein R. The epithelial/carcinoma antigen, EGP-1, recognized by monoclonal antibody RS7-3G11, is phosphorylated on serine 303. *Int J Cancer*. 1995;62:472-479.
- Mansfield E, Amlot P, Pastan I, FitzGerald DJ. Recombinant RFB4 immunotoxins exhibit potent cytotoxic activity for CD22-bearing cells and tumors. *Blood*. 1997;80:2020-2026.
- Soler-Rodriguez A-M, Ghetie M-A, Ghetie N, Openheimer-Marks N, Uhr JW, Vitetta ES. Ricin A-chain and ricin A-chain immunotoxins rapidly damage human endothelial cells: implications for vascular leak syndrome. *Exp Cell Res*. 1993;206:227-234.
- Kuan CT, Pai LH, Pastan I. Immunotoxins containing *Pseudomonas* exotoxin that target Le<sup>y</sup> damage human endothelial cells in an antibody-specific mode: relevance to vascular leak syndrome. *Clin Cancer Res*. 1995;1:1589-1594.
- Vitetta ES, Thorpe PE, Uhr JW. Immunotoxins: magic bullets or misguided missiles. *Trends Pharmacol Sci*. 1993;14:148-154.
- Baluna R, Rizo J, Gordon BE, Ghetie V, Vitetta ES. Evidence for a structural motif in toxins and interleukin-2 that may be responsible for binding to endothelial cells and initiating vascular leak syndrome. *Proc Natl Acad Sci U S A*. 1999;96:3957-3962.
- Newton DL, Hansen HJ, Liu H, et al. Specifically targeting the CD22 receptor of human B-cell lymphoma with RNA damaging agents. *Crit Rev Oncol Hematol*. 2001;39:79-86.
- Onda M, Nagata S, Tsutsumi Y, et al. Lowering the isoelectric point of the Fv portion of recombinant immunotoxin leads to decreased nonspecific animal toxicity without affecting antitumor activity. *Cancer Res*. 2001;61:5070-5077.
- Onda M, Kreitman RJ, Vasmatzis G, Lee B, Pastan I. Reduction of the nonspecific animal toxicity of anti-Tac(Fv)-PE38 by mutations in the framework regions of the Fv which lower the isoelectric point. *J Immunol*. 1999;163:6072-6077.
- Kreitman RJ, Wilson WH, Bergeron K, et al. Efficacy of the anti-CD22 recombinant immunotoxin BL22 in chemotherapy-resistant hairy-cell leukemia. *N Engl J Med*. 2001;345:241-247.